

de Broglie Swapping Metadynamics for Quantum and Classical Sampling

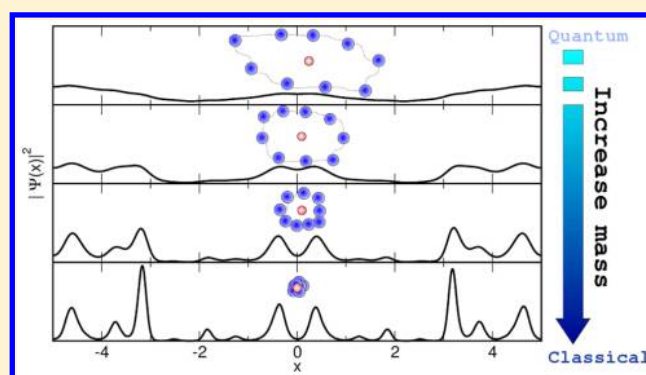
Marco Nava,^{*,†} Ruge Quhe,^{‡,‡} Ferruccio Palazzesi,[†] Pratyush Tiwary,^{§,†} and Michele Parrinello^{*,†}

[†]Department of Chemistry and Applied Biosciences, ETH Zurich, and Facoltà di Informatica, Istituto di Scienze Computazionali, Università della Svizzera Italiana, Via G. Buffi 13, 6900 Lugano, Ticino, Switzerland

[‡]State Key Laboratory of Information Photonics and Optical Communications & School of Science, Beijing University of Posts and Telecommunications, Beijing 100876, China

[§]Department of Chemistry, Columbia University, 3000 Broadway, New York, New York 10027, United States

ABSTRACT: This paper builds on our previous work on Path Integral Metadynamics [Ruge et al. *J. Chem. Theory Comput.* 2015, 11, 1383] in which we have accelerated sampling in quantum systems described by Feynman's Path Integrals using Metadynamics. We extend the scope of Path Integral Metadynamics by combining it with a replica exchange scheme in which artificially enhanced quantum effects play the same role as temperature does in parallel tempering. Our scheme can be adapted so as to be used in an ancillary way to sample systems described by classical statistical mechanics. Contrary to Metadynamics and many other sampling methods no collective variables need to be defined. The method in its two variants, quantum and classical, is tested in a number of examples.



INTRODUCTION

The problem of sampling complex probability distributions is ubiquitous in science. If we focus only on the field of chemistry and physics one of the most serious issues is the presence in many systems of bottlenecks that hinder sampling. From a physical point of view these bottlenecks reflect the existence of metastable states separated by large free energy barriers. Ordinary sampling methods such as Molecular Dynamics (MD) or Monte Carlo are not able to escape the local minimum the simulation was started from.^{1–3}

Over the years many approaches to accelerate sampling in systems described by classical statistical mechanics have been proposed.^{4–12} However, systems in which quantum effects play an important role have received much less attention. Although never explicitly spelled out, two typical quantum effects are expected to help sampling. One is zero point motion that reduces the effective height of the barriers and the other is tunneling across barriers.

A popular computational tool used in the study of quantum effects is the Feynman's path integral (PI) formulation of quantum statistical physics.¹³ If we neglect exchange this leads to an isomorphism in which each quantum particle is mapped into a classical ring polymer of P beads linked by harmonic springs.¹⁴ This description becomes exact for $P \rightarrow \infty$, while $P = 1$ corresponds to the classical limit. By varying P one can go from one regime to another. This formulation allows quantum zero point motion to be easily included, but tunneling, although in principle possible, is difficult to observe^{15,16} if the barriers are high. Here we are not thinking of a method that allows for

calculating transition rates between metastable states once the transition state or the reaction path is known. One can find many such methods in the literature also for quantum systems.^{17–23} Our aim is to design an enhanced sampling method such that during the simulation the system can escape the initial state in an affordable computational time without any knowledge of the transition state or of the new metastable state. Of course, if the barriers are low an enhanced sampling method is not necessary, and barriers can be spontaneously crossed.^{24–26} In a recent paper we have shown in the case of high barriers that progress can be made if we combine PI with Metadynamics¹² in a scheme that we have called PImetaD.²⁷ In this scheme Metadynamics enhances the ring polymer shape fluctuations such that those configurations in which the polymer is stretched from well to well can occur. Those rare fluctuations are precisely those that in the isomorphism allow tunneling to take place.²⁸ The theory of Metadynamics^{29–31} assigns then the correct statistical weight to these conformations. In the same work we have demonstrated the practical usefulness of this approach.

However, in those cases in which transitions involve a complex slow atomic rearrangement also PImetaD has sampling problems. It is one of the objectives of this paper to increase the efficiency of PImetaD. To this effect we take inspiration from parallel tempering³² where M replicas of the system at different temperatures are run in parallel, and

Received: August 26, 2015

Published: October 14, 2015

periodically configurations belonging to neighboring replicas are subject to a Monte Carlo test. If the test is successful the configuration of the two replicas are exchanged. The idea is that at the higher temperatures the system can more easily cross barriers and through the Monte Carlo moves these configurations can be carried down to the lower temperatures. In a similar spirit we shall use quantum effects in a scheme that we call de Broglie replica exchange. We shall run in parallel M copies of the same system. The systems will differ only for the value of their thermal de Broglie wavelength $\lambda = \sqrt{\frac{\beta \hbar^2}{2m}}$. By changing one or more of these parameters one can control the amount of quantum effects. However, changing β toward low temperatures ($\beta \rightarrow \infty$) is not practical. In fact at low temperature the dynamics becomes slower. Thus, the quantity that can be changed is the ratio $\frac{\hbar^2}{m}$. We prefer to express this ratio in terms of the de Broglie wavelength. In the isomorphism the spread of the ring polymer is a measure of its quantum nature, since in a classical system the polymer shrinks to a point. From this point of view λ is the natural unit in which to measure the polymer spread (see eq 4 below).

Thus, in order to enhance quantum effects we shall make the de Broglie lengths of all or part of the system larger than their physical value while keeping the temperature constant. In this way quantum effects will be used to favor barrier crossing. Of course the Monte Carlo swapping test needs to be adapted to this new scheme. We apply successfully this scheme to simple yet challenging quantum systems.

Armed with this new scheme, we shall reconsider the idea of using quantum effects to enhance classical Boltzmann sampling. This idea has been put forward in different contexts by several authors. We quote here the work of the group of Tosatti¹⁶ and that of Berne³³ that uses quantum effects to solve nonlinear optimization problems. Very recently, in a spirit very close to what we are proposing here, Peng et al.³⁴ have presented a quantum replica exchange scheme in which the number of beads P is used to control the amount of quantum effects that is injected into the different replicas. The replica with $P = 1$ is purely classical, and on this replica the statistic is accumulated; the high P replicas are highly quantum and are used to move between different metastable states.

Here we present an alternative to this scheme. We shall keep fixed P and vary the amount of quantum effects in the different replicas by using the de Broglie length and approach the classical limit by reducing the de Broglie length. In addition, taking a cue from the work of Peng et al.,³⁴ we shall add to the quantum replica a classical one decorated with P beads. This last step ensures that we rigorously sample the classical distribution. Using the power of Metadynamics²⁷ we can keep the number of beads low and still induce transitions. Besides the clear computational advantages, this ability to induce fluctuations and tunneling in a system with a limited amount of quantum effects, i.e. small P or small de Broglie length, has the great advantage that even the replica with the highest de Broglie length has a distribution not too distant from the classical one. This circumvents one of the main problems of parallel tempering schemes, namely that often, in order to induce barrier crossing, one has to push the temperature or in this case quantum effects to such a high degree that the system can make an irreversible transition to a new thermodynamic state, for instance a protein can unfold or a solid can melt. Our scheme offers a way of avoiding this problem.

The procedure for sampling classical systems is tested in a 1D glassy system and on alanine dipeptide with comforting results.

METHOD

For simplicity's sake we consider explicitly only the cases in which all the masses are equal

$$\hat{H} = \hat{T} + \hat{V} = -\frac{\hbar^2}{2m} \sum_{i=1}^N \nabla_i^2 + \sum_{i<j}^N V(\hat{r}_{ij}) \quad (1)$$

where m is the mass of the particles, N is the particle number, and \hat{r}_{ij} is the distance between particles i and j . The generalization to systems with different masses is straightforward.

The partition function in the canonical ensemble in the Feynman path integral representation¹³ is

$$Z_\lambda = \lim_{P \rightarrow \infty} \left(\frac{P}{4\pi\lambda^2} \right)^{(dNP)/2} \int \prod_{i=1}^N \prod_{j=1}^P d\vec{r}_{i,j} e^{-\beta A(\{\vec{r}_{i,j}\})} \quad (2)$$

$$A(\{\vec{r}_{i,j}\}) = \sum_{i=1}^N \sum_{j=1}^P \left[\frac{P}{4\beta\lambda^2} (\vec{r}_{i,j+1} - \vec{r}_{i,j})^2 + \frac{1}{P} \sum_{l=i+1}^N V(|\vec{r}_{i,j} - \vec{r}_{l,j}|) \right] \quad (3)$$

where $\vec{r}_{i,P+1} = \vec{r}_{i,1}$, d is the dimensionality of the system, and $\beta = \frac{1}{k_B T}$ its inverse temperature. A is a discretized approximation of the quantum action. This partition function is isomorphic to the configurational integral of a classical system of N ring polymers; each ring polymer is composed of P harmonically interacting beads with a rescaled interpolymer potential $V(r)$ where beads with the same index j can interact.

Sampling Z_λ can be done using a MD simulation. This approach is known in the literature as Path Integral Molecular Dynamics³⁵ (PIMD). Here we focus on MD sampling, but our considerations could be applied to other sampling methods such as Monte Carlo. In order to control the temperature we use a generalized Langevin equation thermostat³⁶ that leads to canonical sampling purposely designed for PI simulations. The need to use this thermostat arises because of the polymer's wide spectrum of mechanical frequencies. In particular the high frequencies of the spectrum couple only very weakly with the slower modes, and if not controlled they behave in a nonergodic manner.³⁷ This method is an alternative to the Normal Mode PIMD method^{38,39} that is usually employed to solve this problem. To avoid confusion we remark that the MD simulation of the ring polymers is used only for sampling and in no way it is meant to approximate real time quantum dynamics as done in ref 40.

In PImetaD, the sampling of the classical system is enhanced using Metadynamics to bias the spring energy collective variable (CV) which in units of $k_B T$ is given by

$$s = \sum_{i=1}^N \sum_{j=1}^P \left[\frac{P}{4\lambda^2} (\vec{r}_{i,j+1} - \vec{r}_{i,j})^2 \right] \quad (4)$$

In ref 27 we have applied with success PImetaD only to cases in which the number of quantum degrees of freedom was small. In order to extend PImetaD to situations in which complex slow degrees of freedom need to be activated for rare state-to-state transitions to be observed we shall introduce two different schemes: one for sampling quantum effects, and the other

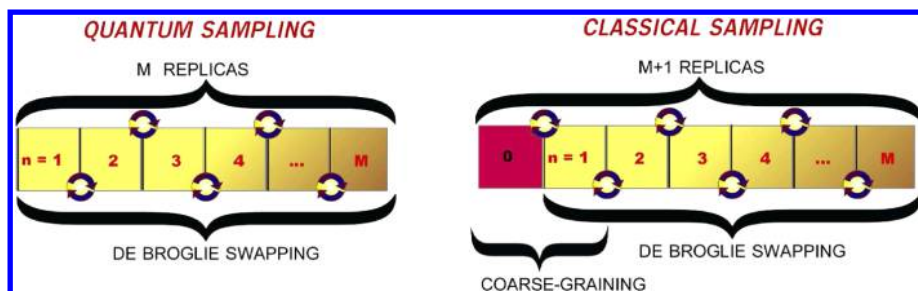


Figure 1. Scheme of dB-PImetaD for quantum sampling (left) and classical sampling (right). Higher n corresponds to replicas with larger de Broglie wavelengths. 0 stands for the coarse-grained replica, where the rigorous classical limit of the sequence is recovered.

instead is to be employed as in ref 34 to sample classical Boltzmann distributions using a chain of artificial quantum systems. In the first case we introduce M replicas, each differing from one another for the value of their de Broglie wavelength λ_n , $n = 1, \dots, M$. The spring elastic energy will be biased as in ref 27. In this case we are interested in the proper quantum description of the system and P has to be taken large enough for the replica that has the physical value of λ to be converged. We shall use the usual Monte Carlo swapping move, which in this case becomes

$$p_{i,i+1} = \min[1, e^{-\beta(\Delta s + \Delta V_b^{(i,i+1)})}] \quad (5)$$

with

$$\Delta s = [s_i(\{R_{i+1}\}) + s_{i+1}(\{R_i\})] - [s_i(\{R_i\}) + s_{i+1}(\{R_{i+1}\})] \quad (6)$$

$$\Delta V_b^{(i,i+1)} = [V_i^{(b)}(s_i(\{R_{i+1}\})) + V_{i+1}^{(b)}(s_{i+1}(\{R_i\}))] - [V_i^{(b)}(s_i(\{R_i\})) + V_{i+1}^{(b)}(s_{i+1}(\{R_{i+1}\}))] \quad (7)$$

since the replica's actions differ only for the value of polymer spring energy and the bias $V_i^{(b)}$. Note that with our choices of using λ to scale the quantum effects the potential energy V cancels out in the Metropolis test. Had we scaled only the temperature as done in parallel tempering this would not have been the case.

If instead our aim is to simulate a classical system the replica exchange scheme can be designed differently. In fact in this case there is no need to describe accurately the quantum system, nor the value of the mass needs to be physical since the classical equilibrium averages of mass-independent operators do not depend on the masses. Thus, we construct a chain of systems that starts from a small value of λ_1 and goes to larger ones. When λ_n is small, the system is almost classical; instead when λ_n is large, quantum effects will be operative. Although the small λ_n replica is very close to a classical system still it is not strictly speaking a classical one. Thus, following the suggestions of Peng et al.³⁴ we add an extra replica defined by a pseudoaction

$$A^{(0)}(\{\vec{r}_{i,j}\}_{i,j}) = \sum_{i=1}^N \sum_{j=1}^P \left[\frac{P}{4\beta\lambda^2} (\vec{r}_{i,j+1} - \vec{r}_{i,j})^2 \right] + \sum_{l < i}^N V(|\vec{r}_i^{(cm)} - \vec{r}_l^{(cm)}|) \quad (8)$$

where $\vec{r}_i^{(cm)} = \frac{1}{P} \sum_{j=1}^P \vec{r}_{i,j}$ is the center of mass. The probability of accepting a swap between replicas 0 and 1 depends on the potential energy and on the bias

$$p_{0,1} = \min[1, e^{-\beta(\Delta V^{(0,1)} + \Delta V_b^{(0,1)})}] \quad (9)$$

$$\Delta V^{(0,1)} = \left[\frac{1}{P} \sum_{j=1}^P \sum_{i < l} V(|\vec{r}_{i,j}^{(0)} - \vec{r}_{l,j}^{(0)}|) + \sum_{i < l} V(|\vec{r}_i^{(cm,1)} - \vec{r}_l^{(cm,1)}|) \right] - \left[\frac{1}{P} \sum_{j=1}^P \sum_{i < l} V(|\vec{r}_{i,j}^{(1)} - \vec{r}_{l,j}^{(1)}|) + \sum_{i < l} V(|\vec{r}_i^{(cm,0)} - \vec{r}_l^{(cm,0)}|) \right] \quad (10)$$

where the superscript 0 identifies a coordinate in the classical replica, the superscript 1 identifies a coordinate in the $n = 1$ replica, and ΔV_b has been defined in eq 7. The overall scheme of dB-PImetaD is reported in Figure 1.

RESULTS AND DISCUSSION

We first study two 1D examples that pose different challenges. One will be treated fully quantum mechanically, while the second is an example of the use of dB-PImetaD to explore classically complex potential energy surfaces *à la Boltzmann*. Later we shall study the alanine dipeptide both in its quantum and classical version.

Quantum One Dimensional Multiwell. In order to illustrate the ability of our scheme to simulate quantum systems

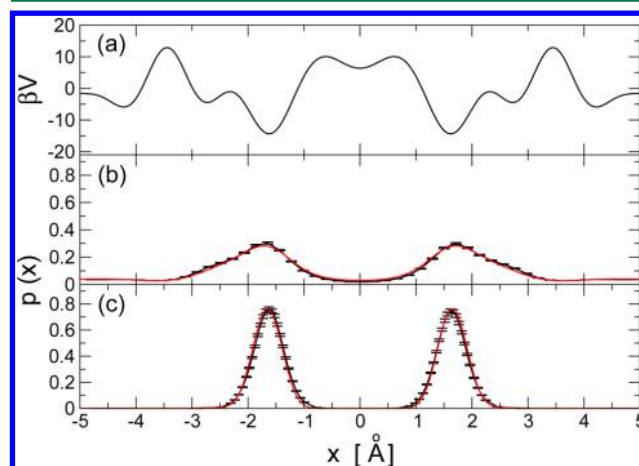


Figure 2. (a) The used external potential. (b) and (c) (black lines) Square modulus of the wave function $p(x)$ for a particle in an external field $V(x)$ at different λ^2 values obtained with dB-PImetaD. The temperature is $T = 1$ K and $P = 40$ beads. (red lines) The numerical solution of the Schrödinger equation in periodic boundary conditions obtained with a plane waves basis set. The simulation consisted of 7 replicas, and the λ^2 values of the shown replicas are 6.072 (b) and 0.607 (c) Å².

we shall first study the multiwell 1D particle in Figure 2 defined by the truncated Fourier series

$$V_{Q1D}(x) = \sum_{j=1}^{10} a_j \cos\left(\frac{2\pi j}{L}x\right) \quad (11)$$

where L is the periodicity, and the coefficients a_j are respectively 1, 3, 8, 0, -2, 0, -5, 0, 2, and -0.6 K. It has two symmetrical minima separated by complex potential barriers. The temperature is $T = 1$ K such that the system is in its ground state. Seven replicas are considered with the values of $\lambda^2 = 0.607, 0.911, 1.202, 1.821, 3.06, 4.554$, and 6.072 \AA^2 . In this as in all the following cases the distance between each consecutive pair of replicas has been set to have approximately the swapping probability of 0.2 which is believed to be optimal.³² A swapping move was attempted every 5 ps, the simulation ran for 100 ns, and the integration time step was 1 fs. The Metadynamics setup consisted of Gaussians with initial amplitude $w_0 = 0.7$ K and $\sigma = 250$ K that were deposited every 4 ps; the bias factor was $\gamma = 9$. The value of P was set to 40 in order to have converged results for all replicas. In the largest λ case the quantum effects alone assisted by PlmetaD were enough to allow tunneling; however, in the smallest λ case crossing the barrier even with PlmetaD would have required impractical long times. The de Broglie swapping scheme instead allows all replicas to be simulated with equal accuracy. In fact all the results are within statistical uncertainty equal to the exact numerical solution of the Schrödinger equation.

Classical One Dimensional Multiwell. We now turn to exemplify the ability of our scheme to sample difficult classical distributions. As a first example we take the same multiwell potential already studied in ref 27. As discussed earlier, in this context we do not need to provide a very accurate description of the quantum system, and thus we have taken $P = 4$. The temperature of the system was chosen to be $T = 0.5$ K, and the replicas are 4 with λ_n^2 values of 0.26, 0.53, and 2.68 \AA^2 . The simulation ran for 6 μs with an integration time step of $dt = 10$ fs. Swap moves were attempted every 4 ps. The initial values of the Metadynamics Gaussian were $w_0 = 0.05$ K and $\sigma = 3$ K, and they were deposited every 2 ps. The bias factor was $\gamma = 1.8$.

The potential in Figure 3 has a multiwell almost glassy character with competing minima separated by high barriers. The absolute energy minimum is at B, while a strong competitor is at A. It is interesting to compare the exact quantum results in the most quantum replica with the $P = 4$ sampling (see Figure 3(b)). The exact quantum result gives a featureless distribution in which the details of the underlying potential are washed out. In contrast in the $P = 4$ calculation a very structured result can be observed, and the density distribution modulations closely reflect that of the potential with maxima at the position of the local potential minima. The most significant remnant of quantum behavior is the fact that the minimum at A appears more populated than the minimum at B. This is due to the sharper curvature of the B minimum that increases locally the zero point motion effects. However, at $\lambda^2 = 0.53 \text{ \AA}^2$ in the fully quantum replica B still is more likely to be occupied but using $P = 4$ it is now A to be lower as in the classical case.

Classical and Quantum Alanine Dipeptide. This small peptide is a classical example on which most sampling methods are tested. Its conformational landscape is well-known and exhibits two basins: a larger and deeper one dominated by the

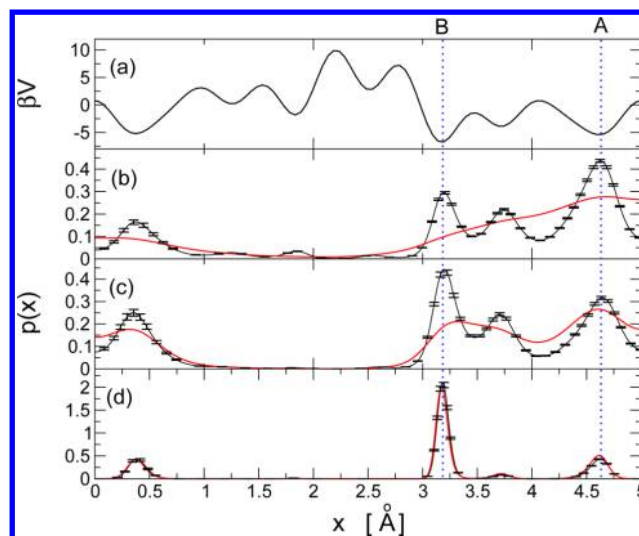


Figure 3. Potential (a) and corresponding logarithm of probability distribution for a particle at $T = 0.5$ K for different λ^2 ((b) and (c)) and for the classical replica (d). The values for λ^2 are in \AA^2 : (b) 2.68 and (c) 0.53. Red lines represent the numerical solution of the Schrödinger equation in periodic boundary conditions. The potential is symmetric around the y axis, and all the results reflect this symmetry within statistical errors.

$C7_{eq}$ and $C5$ conformers with a prevalence of the former and a smaller, higher in energy $C7_{ax}$ conformer.

Since the colored noise thermostat was not designed to deal with rigid bonds we have applied the present methodology to a flexible model using the Charmm22*⁴¹ force field, which is routinely used for small peptides.^{42,43} We have performed an extensive Metadynamics simulation in order to have fully converged results to be used as a benchmark. These results are plotted in Figure 6.

The Metadynamics CVs were the dihedral angles ϕ and ψ (see Figure 4); the parameters were respectively $w_0 = 120$ K

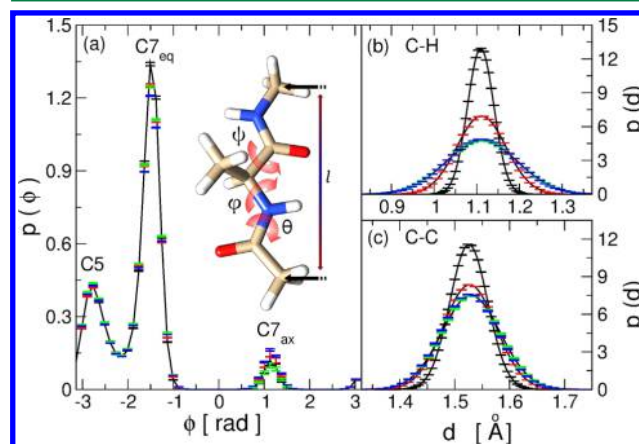


Figure 4. Convergence of some structural properties of alanine dipeptide for different values of P (black for $P = 4$, red for $P = 8$, blue for $P = 16$, and green for $P = 32$) and comparison with the classical results (black error bars): (a) probability distribution of the dihedral angle ϕ , (b) probability distribution for the C-H bond length of one of the methyl groups at the C terminal, and (c) probability distribution for the CO-C $_{\alpha}$ bond length. Black lines are guides to the eye. In the inset: schematic representation of the dihedral angles θ , ϕ , and ψ and the end-to-end distance l .

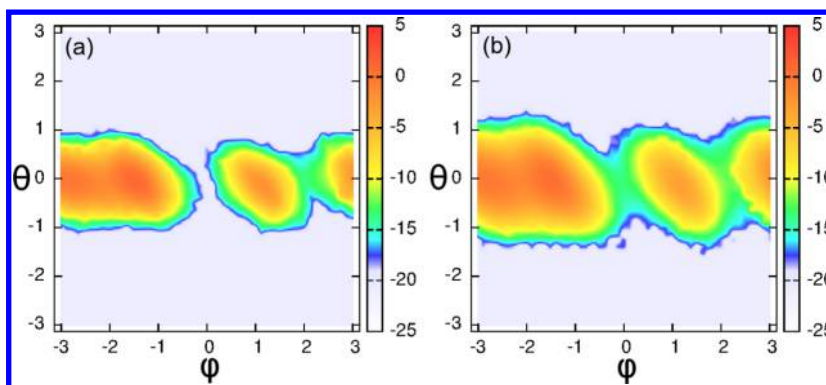


Figure 5. Logarithm of the probability distribution of the dihedral angles θ and ϕ computed with dB-PImetaD for quantum alanine dipeptide. The ratio of the square of de Broglie length of the replicas with respect to that of the first replica, λ_n^2/λ_1^2 are as follows, in \AA^2 : 1.4, 2.5, 4.0, 5.5, 10.0, and 20.0. In (a) is shown the replica with physical de Broglie wavelengths; in (b) is shown the replica with the largest de Broglie wavelengths.

and $\sigma = 0.25$ rad for the Gaussian initial amplitude and standard deviation and $\gamma = 5$ for the bias factor. The Gaussians were deposited every 1 ps. The integration time step was 1 fs, and the simulation was 140 ns long. The simulations were run at 300 K.

We first performed a quantum simulation at different values of P using 7 replicas. The simulations ran for 100 ns, with an integration time step of 1 fs. The bias was built depositing Gaussians of initial amplitude $w_0 = 100$ K and $\sigma = 10000$ K every 2 ps, and the bias factor was $\gamma = 3$. If we were to judge the convergence on the basis of the probability distribution as a function of ϕ , the results would appear to be converged already at $P = 4$ and indistinguishable from the classical result; however, an analysis of other structural properties such as C–C and C–H bond distributions (Figure 4) shows that even at $P = 36$ the results are not yet fully converged and are different from the classical case.

We then asked ourselves what is the mechanism that allows the high λ replicas to make transitions. Since these transitions involve a number of backbone atoms, the effective mass associated with θ , ϕ , and ψ is large, and it is unlikely that tunneling plays a role. Not surprisingly we found this to be the case. In fact if we use ϕ as an order parameter we never find any configuration in which ϕ as a function of the imaginary time index j changes from one well to another. This would have been the signature of a quantum tunneling event.²⁸ We believe instead that due to the fact that quantum fluctuations can stretch or contract the intramolecular bonds the probability of sampling those configurations that eventually lead to conformational changes is enhanced. The transition mechanism for alanine dipeptide has been thoroughly studied by Bolhuis et al.⁴⁴ and more recently by Tiwary et al.,⁴⁵ and it has been found that the transition state ensemble is characterized by an anticorrelation between the angles θ and ϕ . This is seen in Figure 5, where for the replica with largest λ the sampling of the barrier region is clearly enhanced.

The final step in our study of alanine dipeptide was to perform a classical sampling. To this effect we considered first adding to the $P = 4$ replica with physical value of λ 's an extra classical one in the spirit of Peng et al. work³⁴ (see eq 8). Unfortunately the acceptance ratio turned out to be very small indicating that even at $P = 4$ the energy fluctuations did not overlap with those in the classical one. This required adding 8 extra quantum replicas reducing the λ 's from their physical value by as much as a factor 2.88 in the smallest case. The result

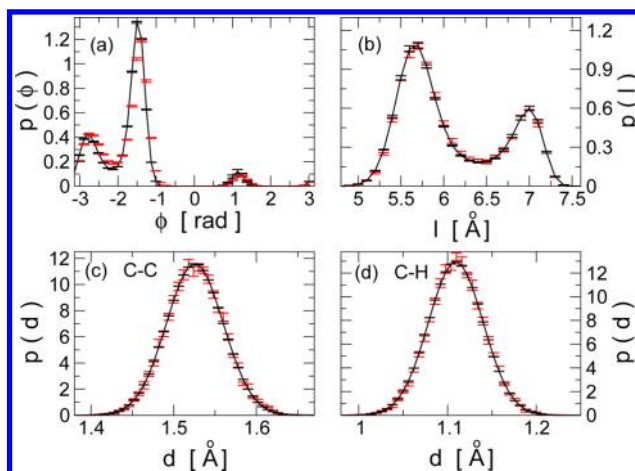


Figure 6. Comparison between a standard Metadynamics simulation and the classical replica of dB-PImetaD for the probability distribution of (a) the dihedral angle ϕ , (b) the end-to-end distance l , (c) the CO–C $_{\alpha}$ distance, and (d) the C–H distance in the methyl group at the C terminal. For dB-PImetaD, the ratio of the square of de Broglie length of the replicas with respect to that of the first replica, λ_n^2/λ_1^2 are as follows, in \AA^2 : 1.4, 1.7, 2.1, 2.7, 4.5, 6.0, 7.7, 10, 15, 26, 41, 80, 140, and 220.

turned out to be identical to the Metadynamics calculation within statistical uncertainties.

CONCLUSIONS

In this work we have extended the applicability of PImetaD obtaining a new approach, dB-PImetaD, that controls the de Broglie wavelength of particles to enhance quantum effects. This method can be used on quantum systems to investigate rare tunneling events. It can also be used to sample classical probability distributions using in the final step a coarse graining of the interaction as similarly done by Peng et al.³⁴

To the best of our knowledge there are no other purposely designed biased sampling methods for quantum systems. In contrast, the literature of enhanced sampling for classical systems is very rich. However, if we compare these methods with ours, we discover that our approach offers several advantages. Contrary to unbiased MD or PIMD it has the ability to overcome large barriers; it does not require the introduction of CVs as in Metadynamics and other similar approaches.^{4,6–8,10–12} Furthermore, one can select only a subset of atoms to be treated as quantum for sampling

purposes, thus enhancing sampling only in targeted regions. This could be very handy for instance in studying conformational transitions in solution or diffusion in solids. Finally, the ability of choosing a low P and still observe transitions due to our brand of Metadynamics allows one to better control the amount of bias in the highly quantum replicas thus avoiding the possibility of inducing unwanted phase transitions as often happens with the standard parallel tempering approach.

Our work is a proof of principle, and there is much room for future improvements. For instance a significant reduction of the computational cost could be achieved by combining it with well tempered ensemble⁴⁶ or with collective variable tempering.⁴⁷ This will lead to a strong reduction in the number of replicas. We shall explore this aspect of our method in the near future.

AUTHOR INFORMATION

Corresponding Authors

*E-mail: mark.nava@gmail.com.

*E-mail: parrinello@phys.chem.ethz.ch.

Notes

The authors declare no competing financial interest.

ACKNOWLEDGMENTS

All calculations were performed on the Brutus HPC cluster at ETH Zurich and on the Rosa supercomputer at the Swiss National Supercomputing Center (CSCS) under project ID u1. We acknowledge the European Union Grant ERC-2009-AdG-247075, Marvel 51NF40_141828, and the China Scholarship Council for funding.

REFERENCES

- (1) Copeland, R. A.; Pompliano, D. L.; Meek, T. D. *Nat. Rev. Drug Discovery* **2006**, *5*, 730.
- (2) Nuñez, S.; Venhorst, J.; Kruse, C. G. *Drug Discovery Today* **2012**, *17*, 10.
- (3) Davey, R. J.; Schroeder, S. L. M.; ter Horst, J. H. *Angew. Chem., Int. Ed.* **2013**, *52*, 2166.
- (4) Torrie, G.; Valleau, J. P. *J. Comput. Phys.* **1977**, *23*, 187.
- (5) Wang, F.; Landau, D. P. *Phys. Rev. Lett.* **2001**, *86*, 2050.
- (6) Darve, E.; Pohorille, A. *J. Chem. Phys.* **2001**, *115*, 9169.
- (7) Maragliano, L.; Vanden-Eijnden, E. *Chem. Phys. Lett.* **2006**, *426*, 168.
- (8) Maragakis, P.; van der Vaart, A.; Karplus, M. *J. Phys. Chem. B* **2009**, *113*, 4664.
- (9) Bowman, G. R.; Beauchamp, K. A.; Boxer, G.; Pande, V. S. *J. Chem. Phys.* **2009**, *131*, 124101.
- (10) Bolhuis, P. G.; Chandler, D.; Dellago, C.; Geissler, P. L. *Annu. Rev. Phys. Chem.* **2002**, *53*, 291.
- (11) Laio, A.; Parrinello, M. *Proc. Natl. Acad. Sci. U. S. A.* **2002**, *99*, 12562.
- (12) Barducci, A.; Bussi, G.; Parrinello, M. *Phys. Rev. Lett.* **2008**, *100*, 020603.
- (13) Feynman, R. P.; Hibbs, A. R. *Quantum Mechanics and Path Integrals*; McGraw-Hill Companies: New York, 1965.
- (14) Parrinello, M.; Rahman, A. *J. Chem. Phys.* **1984**, *80*, 860.
- (15) Stella, L.; Santoro, G. E.; Tosatti, E. *Phys. Rev. B: Condens. Matter Mater. Phys.* **2006**, *73*, 144302.
- (16) Santoro, G. E.; Tosatti, E. *J. Phys. A: Math. Gen.* **2006**, *39*, R393.
- (17) Gao, J.; Wong, K.-Y.; Major, D. T. *J. Comput. Chem.* **2008**, *29*, 514.
- (18) Wong, K.-Y.; Gao, J. *J. Chem. Phys.* **2007**, *127*, 211103.
- (19) Wong, K.-Y.; Gao, J. *J. Chem. Theory Comput.* **2008**, *4*, 1409.
- (20) Voth, G. A.; Chandler, D.; Miller, W. H. *J. Chem. Phys.* **1989**, *91*, 7749.
- (21) Craig, I. R.; Manolopoulos, D. E. *J. Chem. Phys.* **2005**, *122*, 084106.
- (22) Richardson, J. O.; Althorpe, S. C. *J. Chem. Phys.* **2009**, *131*, 214106.
- (23) Vanicek, J.; Miller, W. H.; Castillo, J. F.; Aoiz, F. J. *J. Chem. Phys.* **2005**, *123*, 054108.
- (24) Gillan, M. J. *Phys. Rev. Lett.* **1987**, *58*, 563.
- (25) Kretchmer, J. S.; Miller, T. F., III. *J. Chem. Phys.* **2013**, *138*, 134109.
- (26) Wong, K.-Y.; Richard, J. P.; Gao, J. *J. Am. Chem. Soc.* **2009**, *131*, 13963.
- (27) Quhe, R.; Nava, M.; Tiwary, P.; Parrinello, M. *J. Chem. Theory Comput.* **2015**, *11*, 1383.
- (28) Chandler, D.; Wolynes, P. G. *J. Chem. Phys.* **1981**, *74*, 4078.
- (29) Dama, J. F.; Parrinello, M.; Voth, G. A. *Phys. Rev. Lett.* **2014**, *112*, 240602.
- (30) Tiwary, P.; Parrinello, M. *J. Phys. Chem. B* **2015**, *119*, 736.
- (31) Bonomi, M.; Barducci, A.; Parrinello, M. *J. Comput. Chem.* **2009**, *30*, 1615.
- (32) Swendsen, R. H.; Wang, J. S. *Phys. Rev. Lett.* **1986**, *57*, 2607.
- (33) Liu, P.; Berne, B. J. *J. Chem. Phys.* **2003**, *118*, 2999–3005.
- (34) Peng, Y.; Cao, Z.; Zhou, R.; Voth, G. A. *J. Chem. Theory Comput.* **2014**, *10*, 3634.
- (35) Berne, B. J.; Thirumalai, D. *Annu. Rev. Phys. Chem.* **1986**, *37*, 401.
- (36) Ceriotti, M.; Parrinello, M.; Markland, T. E.; Manolopoulos, D. E. *J. Chem. Phys.* **2010**, *133*, 124104.
- (37) Hall, R. W.; Berne, B. J. *J. Chem. Phys.* **1984**, *81*, 3641.
- (38) Cao, J.; Berne, B. J. *J. Chem. Phys.* **1993**, *99*, 2902.
- (39) Cao, J.; Martyna, G. J. *J. Chem. Phys.* **1996**, *104*, 2028.
- (40) Habershon, S.; Manolopoulos, D. E.; Markland, T. E.; Miller, T. F., III. *Annu. Rev. Phys. Chem.* **2013**, *64*, 387.
- (41) Piana, S.; Lindorff-Larsen, K.; Shaw, D. E. *Biophys. J.* **2011**, *100*, L47.
- (42) Palazzesi, F.; Prakash, M. K.; Bonomi, M.; Barducci, A. *J. Chem. Theory Comput.* **2015**, *11*, 2.
- (43) Lindorff-Larsen, K.; Maragakis, P.; Piana, S.; Eastwood, M. P.; Dror, R. O.; Shaw, D. E. *PLoS One* **2012**, *7*, e32131.
- (44) Bolhuis, P. G.; Dellago, C.; Chandler, D. *Proc. Natl. Acad. Sci. U. S. A.* **2000**, *97*, 5877.
- (45) Tiwary, P.; Parrinello, M. *Phys. Rev. Lett.* **2013**, *111*, 230602.
- (46) Bonomi, M.; Parrinello, M. *Phys. Rev. Lett.* **2010**, *104*, 190601.
- (47) Gil-Ley, A.; Bussi, G. *J. Chem. Theory Comput.* **2015**, *11*, 1077.